JOURNAL OF MATERIALS SCIENCE 2 (1967) 444–456

Rare-Gas Mobility in Some Anisotropic Ceramic Oxides: Al_2O_3, Cr_2O_3, Fe_2O_3, TiO_2, U_3O_8

Hj. MATZKE
Laboratory for Nuclear and Radiochemistry, Technical University, Braunschweig, Germany

Received 8 May 1967

The mobility of the inert gases xenon or radon in five anisotropic oxides (hexagonal corundum Al_2O_3, Cr_2O_3, Fe_2O_3, tetragonal rutile TiO_2, and orthorhombic U_3O_8) was studied. The gases were introduced by ion bombardment. The oxides were in the form of powders, sinters, or single crystals. Normal volume diffusion was found at low gas concentration, the activation energies in kilocalories per mole being $\geqslant 85$ for Al_2O_3, 73 ± 5 for Cr_2O_3, 68 ± 5 for Fe_2O_3, 78 ± 5 for TiO_2, and 85 ± 8 for U_3O_8, and the pre-exponential terms D_0 falling into the "ideal" range of about $3 \times 10^{-1} \pm 1$ cm^2/sec. Structural radiation damage, the annealing of which coincided with gas release at low temperatures, and, in some cases, retardation of the gas release were found at higher gas concentrations. Some evidence is presented that grain boundaries, pre-existing vacancy clusters, and dislocation loops may act as trapping sites for gas atoms (or bubbles) and may be stabilised after trapping of the gas.

1. Introduction

The technique of ion bombardment provides a good means of studying the various factors and experimental conditions affecting inert-gas mobility in solids. By using isotope separation, the bombardment dose is readily varied by many orders of magnitude. Thus, the effects of gas concentration and of various types of radiation damage on gas release can easily be studied.

Previous work on a variety of ionic crystals and sinters has shown that volume diffusion occurring at *normal* temperatures (i.e. starting at roughly 0.4 to 0.5 of the melting point on the absolute temperature scale) is generally characteristic of low bombardment doses. At high doses, release is either connected with the annealing of structural radiation damage and occurs at *low* temperatures, or else trapping of gas in irradiation-induced defects or gas/gas interactions retard the release which thus does not start before *high* temperatures are reached.

Most gas diffusion work on ionic crystals and sinters has been done using cubic materials with the fluorite or rocksalt structures, mostly because their basic physical properties are better understood and also because of the importance of the ceramic fuel materials UO_2 and UC which exhibit these lattice structures, and in which inert gases are formed as fission products. (The problems connected with the mobility of such gases to form bubbles have been the main motive for the study of inert-gas diffusion.) Some non-cubic materials, however, have also been studied. Here, the influence of gas concentration, and hence radiation damage, is especially important because of the lower stability of the lattice. In the present study, five anisotropic oxides (Al_2O_3, Fe_2O_3, Cr_2O_3, TiO_2, U_3O_8) are investigated. As no clear decision could be made concerning the nature of lattice disorder in these substances*, or because the binding was not well understood, doping was considered to be less helpful for the study of the mechanism of gas release than it was with materials having types of disorder which are well understood (e.g. UO_2 [1], ThO_2 [2], CaF_2

*i.e. the nature of the point defects and their distribution among the sub-lattices

TABLE I Description of specimens.

Al_2O_3	Corundum (sapphire)	Single crystal	Linde, New York
	α-phase	Powder	Degussa, Hanau, surfaces 51 and 100 m^2/g
	,,	Powder	Merck "Brockmann", 50 μm diameter
Cr_2O_3		Sinter	AECL, pressed with 40 000 lb/in.²*, sintered at 1500° C
Fe_2O_3		Sinter	AECL, pressed with 40 000 lb/in.², sintered at 1500° C
TiO_2	Rutile	Single crystal	Semi Elements Inc, Saxonburg, Pa, USA
		Powder	Merck "pro analysi", surface 10.5 m^2/g
U_3O_8		Sinter	AECL, pressed with 40 000 lb/in.², sintered at 1100° C
		Powder	AB Atomenergi, Sweden

All samples were annealed for several hours to the highest temperatures used for diffusion studies before introducing the gas.

*1 lb/in.^{2} = 7×10^{-2} kg/cm^2

[3, 4], or KBr [5]). Instead, advantage was taken of the possibility of producing structural radiation damage [6] or non-stoichiometry (with rutile), and thus of obtaining lattice imperfections of different kinds which are expected to influence the release behaviour.

A system of numbered stages has been introduced [7, 8] to describe conveniently gas release processes. In the present work, the main emphasis will be put on normal volume diffusion, or stage II. Stage I, or "low-temperature gas release", using the same oxides, is described elsewhere [4, 9, 10]. Stage III, or "strong trapping", is studied here by using material with pre-existing defects such as grain boundaries, vacancy clusters, and dislocation loops, and in comparison with material which does not contain these defects. Evidence will be advanced that: (i) the above-mentioned defects may act as trapping sites owing to a *strong* gas/defect interaction; (ii) radiation-induced defects may provide trapping sites for *weak* gas/defect interaction and thus lead to a retarded gas release rather than to permanent trapping.

2. Materials

The materials used, either single crystals and sinters of approximately $5 \times 5 \times 1$ mm size, or powders, are described in table I.

Rutile was used both in stoichiometric and in reduced form. The reduction was carried out in vacuum or hydrogen and controlled by following the weight loss. Reduction of TiO_2 starts at about 300° C in reducing atmospheres or vacuum, and at about 800° C in air. The range of homogeneity for the rutile phase is very narrow: at 1100° C the limits are $TiO_{1.991}$ to TiO_2 [11-13]. Heating in hydrogen or vacuum at temperatures in excess of 1100° C leads to the formation of new phases. For instance, X-ray determinations following reductions at 1350° C for 1 h showed the presence of Ti_3O_5. Reheating the samples in air leads back to stoichiometry at about 800° C.

3. Experimental

The experimental details have been reported elsewhere [5]. For *labelling* with argon or xenon, single crystals or sinters were bombarded in the Chalk River mass separator using 40 keV ions and different bombardment doses: low doses of 8×10^{10} to 1×10^{11} ions/cm^2, intermediate doses of 4×10^{13} to 4×10^{14} ions/cm^2, and high doses of 5×10^{15} to 2×10^{16} ions/cm^2. Different isotopes were used to achieve these doses. Labelling of powders with radon was done using a technique developed previously [14]. About 3×10^{-4} mg radium were adsorbed on the powders from an aqueous $RaCl_2$ solution. The daughter-product Rn^{222} was recoiled into the powders by the recoil energy of about 85 keV originating from the α-decay. After about one week's exposure, the residual Ra^{226} was washed off in hot 0.1 M HCl or HNO_3. By following the decay of the radioactivity, it was shown that no radium had remained on the oxide powders as the half-life corresponded to that of Rn^{222} (3.82 days).

Annealing in air was performed in a wire-wound tube furnace; hydrogen (360 torr), nitrogen and vacuum annealings (about 10^{-5} torr) were done in a molybdenum-tube resistance furnace as described by MacEwan [15]. The annealing time in taking F/T curves* (isochronal annealings) was always 5 min at each temperature at intervals of 75 to 100° C. Iso-

*F represents the fraction of gas which has been released.

thermal experiments were carried out at various temperatures for periods of up to several days.

Counting of radioactive xenon and argon was done at the bombarded surfaces of the samples using a flow-type proportional counter. Radon was measured in the gas phase using the counting equipment described previously [14]: a gas stream was led over the sample, was purified of solid decay products by passing through sieves, and the radon concentration was counted in a separate chamber provided with a CsI-scintillation crystal. The total activity of radon was determined by raising the sample temperature until all the radon was released into the gas phase, which was in turn confirmed by noting the absence of the (β, γ)-activity of the daughter products of radon at the sample after reaching equilibrium (about 8 h).

4. Analysis

The solutions of the diffusion equation needed for analysis of the xenon release data have been given before [5, 16]. Two different approaches were used.

(*a*) Activation enthalpies ΔH were derived from the release temperatures assuming an idealised range of values for D_0 of $3 \times 10^{-1\pm1}$ cm^2/sec which agrees best with reliable literature data (see reference 16 for details).

(*b*) ΔH and D_0 were derived independently from the measured release curves (see reference 5 for details).

In the case of α-recoil labelling of powders (particle radius $a \leqslant 2\ R_m$; R_m = median range of the ions), the fractional release expression for spherical geometry was used [8, 14] as a good approximation even for $a \approx 2R_m$. It has been shown [17] that the shape of the general release curve for a sphere is largely independent of the ratio of a/R_m for the interval $R_m \leqslant a \leqslant 2R_m$. By using a semi-infinite instead of a spherical geometry, one would obtain too high values of D at higher temperatures.

5. Results

5.1. Corundum, α-Al_2O_3

Figs. 1 to 3 show the release of rare gases from α-Al_2O_3 single crystals and powders. In fig. 1, two isothermal release curves of α-recoil radon from Al_2O_3 powders are given together with a third curve for the release of xenon from a single crystal following ion bombardment to 8×10^{10} ions/cm^2. In all three cases, the release can be fitted to curves representing the theoretical release expressions [5, 14, 17]. The difference in shape between release curves for powders and single crystals is due to the fact that the latter have to be regarded as semi-infinite and thus show the influence of some diffusion into the bulk of the sample.

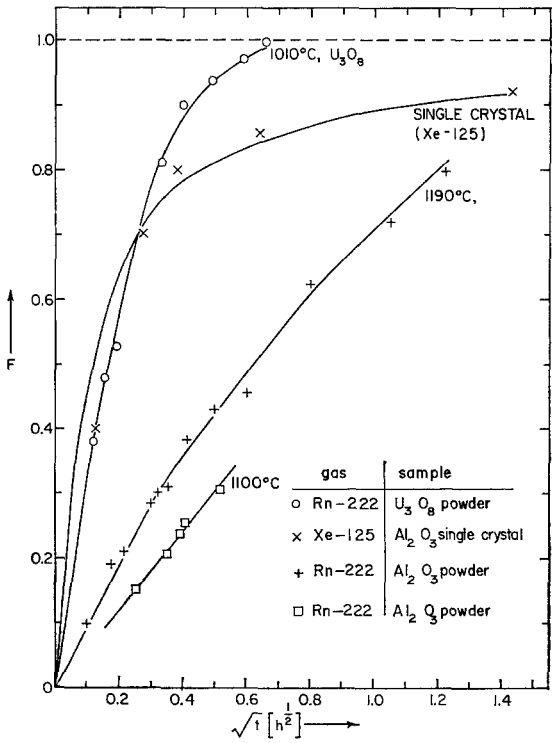

Figure 1 Release of radon from Al_2O_3 (10^4 ions/cm^2) and U_3O_8 powders (10^8 ions/cm^2) and release of xenon (8×10^{10} ions/cm^2) from single crystalline Al_2O_3 (the latter at 1300°C). The curves represent the theoretical release expressions [5] for varying D/R^2_m. (F represents the fraction of gas released.)

Diffusion coefficients for radon, calculated from isothermal release curves obtained with powders of three different grain sizes and with three different annealing atmospheres, are plotted in an Arrhenius diagram in fig. 2. For comparison, results for self-diffusion of aluminium [18] and oxygen [19] in α-Al_2O_3 are reproduced in fig. 2 together with two sets of results [20] for fission-recoil xenon (broken lines a and b). The radon diffusion coefficients scatter around two curves according to the respective surface areas (55 or 100 m^2/g) of the powders; this may be due to errors in the determination of the surface areas, which was done using the

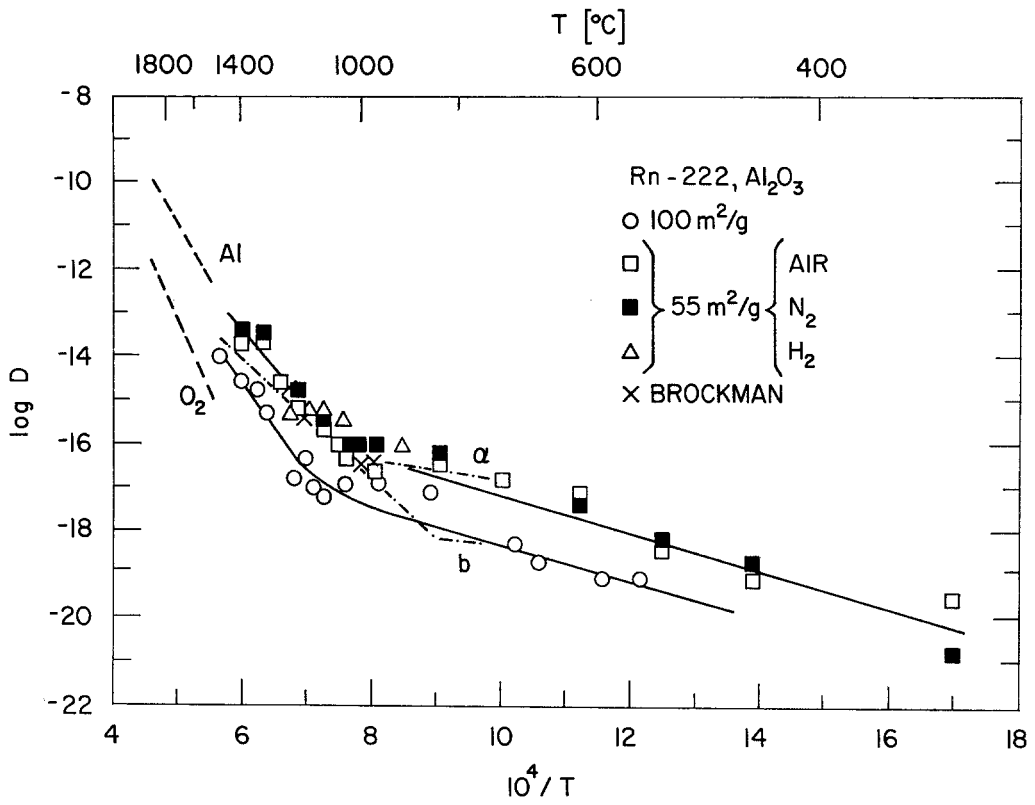

Figure 2 Arrhenius plot for the release of radon from three different Al_2O_3 powders heated in different atmospheres (air, N_2, H_2). Included are results for self-diffusion of aluminium [18] and oxygen [19]. Curves a and b represent release of fission xenon [20].

BET method*. The slopes of the two curves, however, are nearly identical. Both curves consist of two approximately straight lines showing a low-temperature process with an apparent activation enthalpy ΔH of about 21 kcal/mole up to about 1100° C, and a high-temperature process which can be described with $\Delta H = 80$ to 85 kcal/mole and $D_0 = 0.03$ to 0.18 cm^2/sec. No obvious effect of heating atmosphere (air, H_2, N_2) on radon release was observed. A part of the results given here has been published previously [14]; it yielded a slightly lower ΔH owing to a smaller number of experiments.

Fig. 3 shows F/T curves for the release of rare gases from α-Al_2O_3. At high doses of 2×10^{16} ions/cm^2, an abnormal low-temperature release at 650 ± 50° C is noticed (curves 1). This release was first observed for krypton bombardment [8] and later found [6] to coincide with the annealing of structural radiation damage. High-dose ion bombardment was shown to cause a phase change to a quasi-amorphous phase; the recrystallisation (i.e. the amorphous/crystalline transition) occurred at 650 ± 50° C and thus coincided with this gas release [6]. Low-dose bombardment [8] with α-recoil radon (1 to 2×10^4 ions/cm^2) is represented in curve 2 taken from reference 8, yielding $\Delta H = 95 \pm 5$ kcal/mole by using approach (*a*) given in section 4. For xenon bombardment to a low or an intermediate dose of 8×10^{10} or 4×10^{13} ions/cm^2, a ΔH of 97 ± 5 kcal/mole (approach (*a*)) is obtained. Approach (*b*), however, results in $\Delta H = 130 \pm 10$ kcal/mole and a high D_0 of $10^{5.5 \pm 0.5}$ cm^2/sec for the xenon data. With a further increase of the xenon concentration to about 4×10^{14} ions/cm^2, the release is shifted to still higher temperatures. No obvious effect of heating atmosphere (air, H_2) on xenon release is observed. At a few temperatures, the release of argon was measured (curve 6). No essential

*S. BRUNAUER, P. H. EMMETT, and E. TELLER, *J. Amer. Chem. Soc.* **60** (1938) 309.

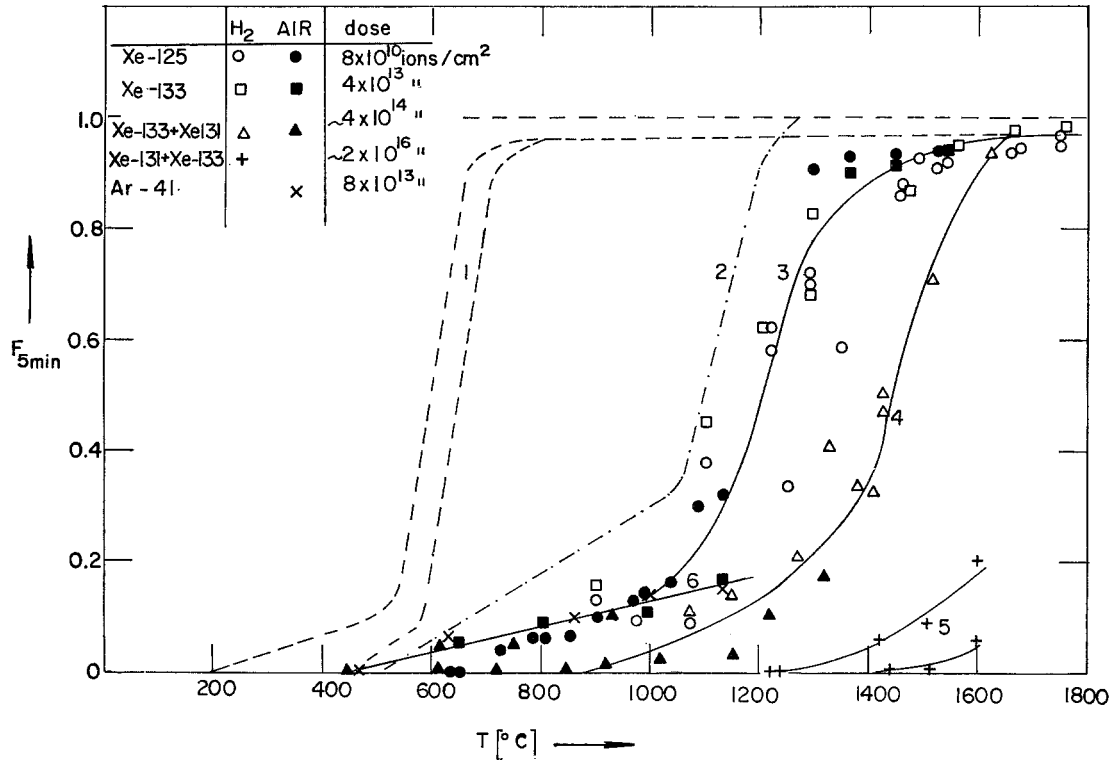

Figure 3 Release of rare gases from Al_2O_3 single crystals during heating in air or hydrogen. (F_{5min} represents the gas fraction released during 5 min of annealing.) Curves 1 are taken from reference 6 and represent the release of xenon and krypton at a high dose of 1×10^{16} to 2×10^{16} ions/cm^2. Curve 2 is taken from reference 8 and represents the release of radon from Al_2O_3 powders at a very low dose of 10^4 ions/cm^2. Curve 5 refers to a double gas-charging treatment (see text). Curve 6 represents some release experiments with Ar^{41}.

difference compared with the release of xenon was found.

Some crystals were first bombarded with 4×10^{13} Xe^{133} ions/cm^2. Following this bombardment, a phase change was produced within a thin surface layer by bombarding with 2×10^{16} Xe^{131} ions/cm^2, which have a smaller range owing to the high gas concentration [6]. At $650 \pm 50°$ C, the reported phase change to polycrystallinity occurred, providing a surface layer containing small grains and grain boundaries. During this phase change, about 95% of the Xe^{131} and about 30% of the Xe^{133} escaped. Subsequent release did not start until temperatures in excess of 1200° C were reached (curve 5).

5.2. Cr_2O_3 and Fe_2O_3

Fig. 4 shows the release of xenon from Cr_2O_3 sinters for various bombardment doses. For the low dose of 8×10^{10} and the intermediate dose of 4×10^{13} ions/cm^2, a release (curve 3) compatible with a single activation enthalpy ΔH of 73 ± 5 kcal/mole is found. However, release does not go to completion even on increasing the temperature to 1400° C. At high doses of 5×10^{15} (curve 2) or 2×10^{16} ions/cm^2 (curve 1), release is shifted to markedly lower temperatures. Reflection electron diffraction patterns of the bombarded surface layers showed that a partial phase change to a quasi-amorphous phase was caused by the high-dose bombardment. One of these partly amorphous samples was annealed at 1050° C and showed the original diffraction pattern, indicating complete recrystallisation.

In fig. 5, the release of xenon from Fe_2O_3 sinters and the release of radon from Fe_2O_3 powder is shown. Curves 3 and 4b are compatible with single activation enthalpies of 68 ± 5 and 78 ± 5 kcal/mole respectively.

At increased doses, release is shifted to lower temperatures. A small effect is already observed for the intermediate dose of 4×10^{13} ions/cm^2.

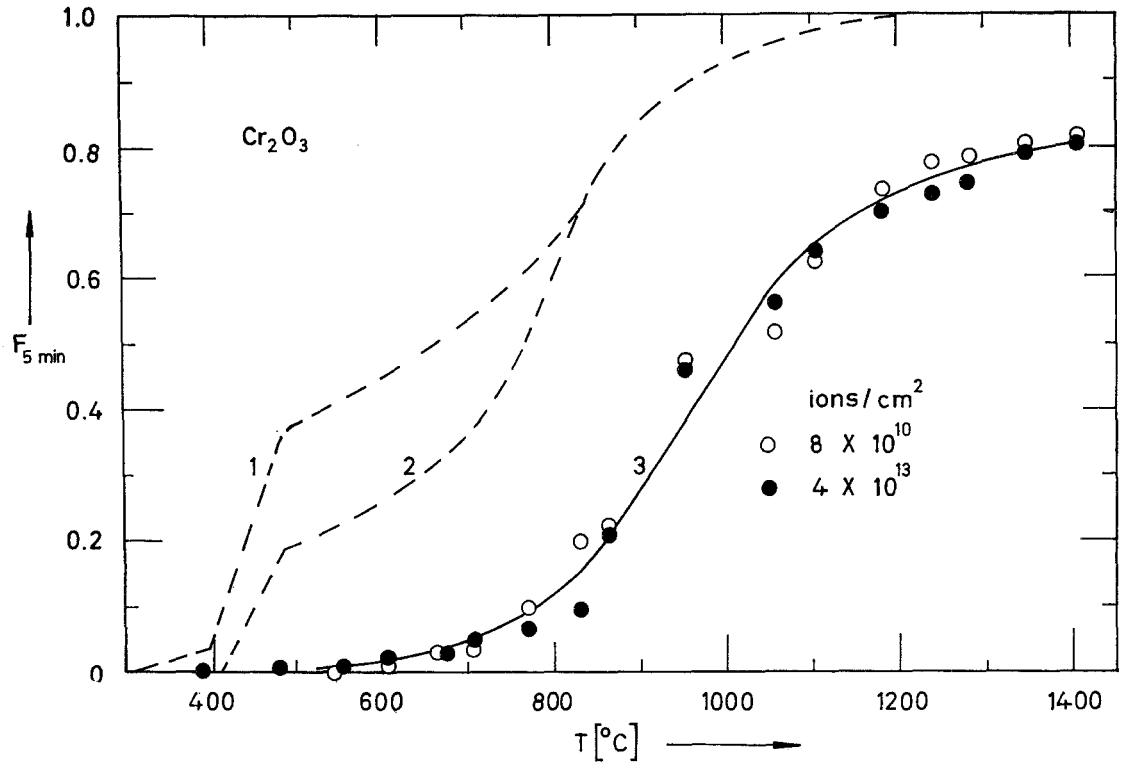

Figure 4 Release of xenon from Cr_2O_3 sinters. Curves 1 and 2 represent release at high doses of 2×10^{16} and 5×10^{15} ions/cm^2 respectively [4].

For the dose of 5×10^{15} ions/cm^2 (curve 2) and of 2×10^{16} ions/cm^2 (curve 1), release is shifted to still lower temperatures. As with Cr_2O_3, reflection electron diffraction pattern of the bombarded surfaces indicated a partial phase change to a quasi-amorphous phase, and recrystallisation was completed at 1050° C.

5.3. Rutile, TiO_2

Fig. 6 shows the release of xenon from stoichiometric and sub-stoichiometric single crystalline TiO_2 and the release of radon from TiO_2 powders. A release component at low temperatures (approx. $\leqslant 0.5\ T_m = 780°$ C) is found in all cases, but this component is much greater after high-dose bombardment, which causes a phase change to a quasi-amorphous phase [6]. The release of curve 4 has been shown to coincide with the recrystallisation of the damaged sample [6].

The low-dose radon data (curve 1, approx. 10^5 ions/cm^2) are compatible with a single activation enthalpy ΔH of 78 ± 5 kcal/mole. The release of xenon at doses of 8×10^{10} and 4×10^{13} ions/cm^2 occurs at higher temperatures (curve 2). A small effect of dose is indicated: release at the higher dose leads to slightly lower F-values at practically all temperatures above those of the low-temperature release.

Annealing of stoichiometric rutile in hydrogen leads to enchanced release connected with reduction *during* the diffusion experiments [6]. This is indicated both by the single point for Xe^{133} ($F = 0.98$, $T = 835°$ C) which was obtained in triplicate, and by the coincidence of the data for rutile with Xe^{125}, annealed in hydrogen, with curve 1 rather than curve 2.

On the other hand, reduction of the material before bombardment, and hence *before* the diffusion experiment, leads to retention of the gas up to high temperatures, as indicated by comparing curves 2 and 3. For curve 3, single crystals were reduced to TiO_{2-x} *before* bombardment. The diffusion experiments were done in air. Thus, oxidation to TiO_2 is expected to be completed at about 800° C (see section 2).

5.4. U_3O_8

Fig. 1 shows the isothermal release of radon from U_3O_8 powder at 1010° C. The release fol-

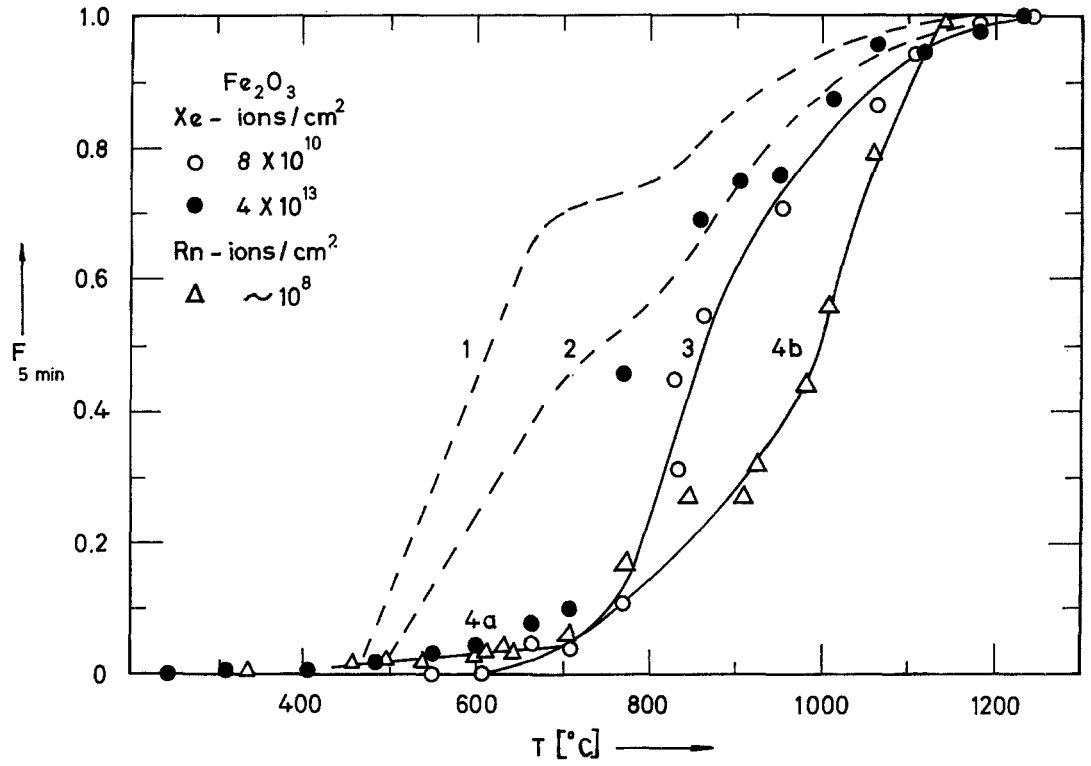

Figure 5 Release of xenon from Fe_2O_3 sinters and release of radon from Fe_2O_3 powder. Curves 1 and 2 represent xenon release at high doses of 2×10^{16} and 5×10^{15} ions/cm² respectively [4].

lows the theoretically expected curve. Fig. 7 contains isochronal release curves for the release of xenon from U_3O_8 sinters following bombardment to low or intermediate doses of 8×10^{10} or 4×10^{13} ions/cm², and for the release of radon from U_3O_8 powders following labelling with low doses of 10^8 and 2×10^{10} ions/cm². In reference 6, it was reported that, even with the low dose used for xenon bombardments (8×10^{10} ions/cm²), the bombarded surface layers are rendered quasi-amorphous. The subsequent release occurs, therefore, from amorphous material which recrystallises during the temperatures of gas release. Thus, evaluation of diffusion constants will not yield values representative for pure diffusion in crystalline U_3O_8, and the values obtained from curve 1 ($\Delta H = 74 \pm 5$ kcal/mole, $D_0 = 0.05 \pm 0.03$ cm²/sec) may be assumed to be low.

The data for radon release following bombardment to 2×10^{10} ions/cm² coincide with the xenon data. However, for a very low dose of about 10^8 ions/cm², a separate release curve at higher temperatures is obtained (curve 2) which yields a ΔH of 89 ± 5 kcal/mole and D_0 of $3 \times 10^{0 \pm 0.5}$ cm²/sec. No electron diffraction analysis for determining structural radiation damage could be made as the specimens used for radon release experiments were powders. However, this ΔH is probably as close to the true value as it is possible to come, given the great tendency of U_3O_8 to become amorphous.

6. Discussion

6.1. Corundum, α-Al_2O_3

The present work shows that several different processes contribute to the gas release from α-Al_2O_3, the relative proportions of which depend on bombardment energy and dose (gas concentration). The radon data represent high-energy and low-dose bombardments. At temperatures in excess of 1000 to 1100° C ($\approx 0.55\ T_m$), the isothermal release curves for radon (fig. 1) follow the theoretical expression; the release temperatures are compatible with the rate of self-diffusion (fig. 2) and the D_0 has an ideal value near unity. These results are in favour of a volume diffusion process which is not perturbed by gas concentration or radiation damage; thus, if the gas is dissolved atomically, the mobility would involve jumps of the gas atoms *amongst* equilibrium vacancies (the

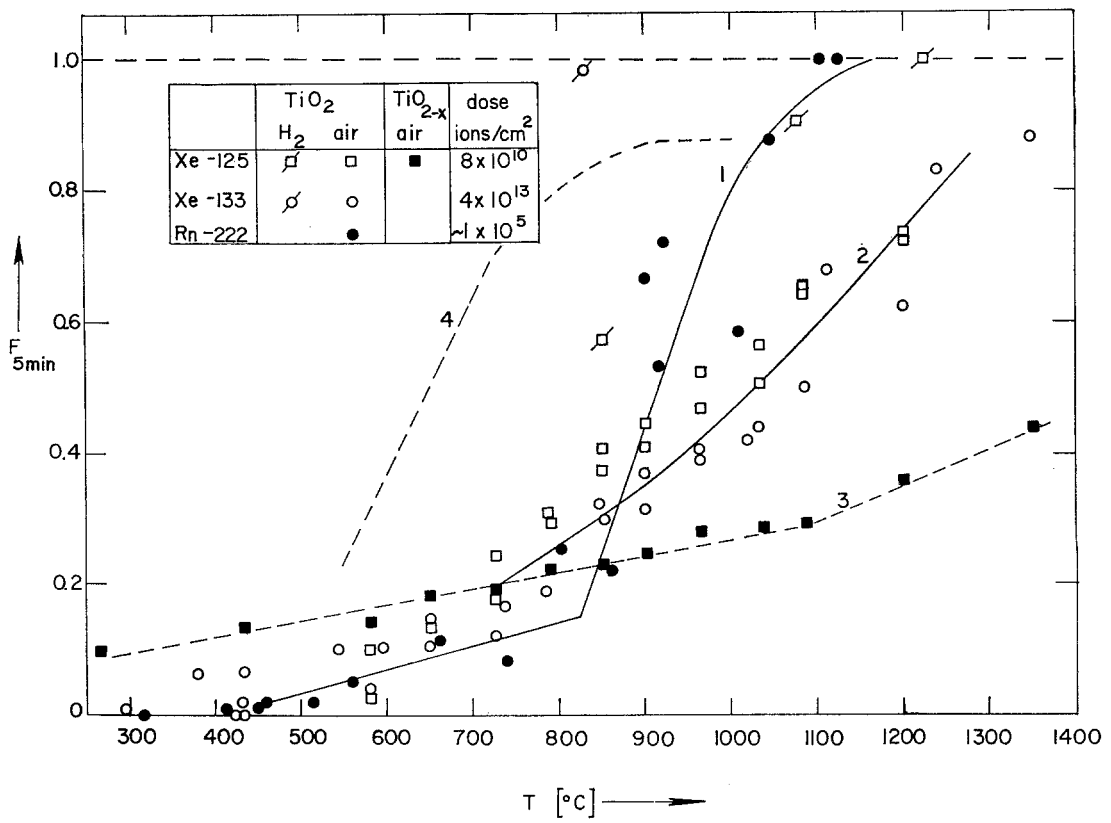

Figure 6 Release of xenon from rutile single crystals and release of radon from rutile powder. Curve 4 is taken from reference 6 and represents xenon release at a high dose of 2×10^{16} ions/cm^2.

mechanism would be somewhat different if the gas sits in a small equilibrium vacancy cluster, as is indicated for xenon diffusion in UO_2 [1], ThO_2 [2], and KBr [5]. Neither of these possibilities can be favoured, as nothing is known about the solubility of heavy rare gases in α-Al_2O_3, nor has the nature of the lattice disorder of α-Al_2O_3 been determined as yet: both Schottky disorder (vacancies in both cation and anion sub-lattices) and Frenkel disorder (aluminium vacancies and interstitials) have been suggested.

Stage I release at high doses (coinciding with the amorphous/crystalline transition) or low energies (connected with surface proximity of the gas) has been discussed previously [6, 7, 9, 10]. Some new indication of low-temperature release for argon and xenon has been found in the present work (curve 6 of fig. 3). This release may possibly be due to formation of some damage and its annealing, or else to surface proximity of some gas.

The present work puts more emphasis on high-temperature processes (i.e. processes occurring at temperatures in excess of those of volume diffusion). These releases are difficult to observe with α-Al_2O_3, since at high doses the quasi-amorphous phase is formed and most of the label is lost during the amorphous/crystalline transition. Fig. 3 shows that a gradual increase in gas concentration leads first to a shift of gas release to higher temperatures (i.e. a retardation of gas release – curves 2, 3, and 4), until the bombardment dose is high enough to produce the phase change (curves 1). This shift in temperature implies the existence of *weak* trapping (weak gas/gas or gas/defect interaction). Similar indications for weak trapping have been observed for a variety of materials including UO_2 [1], ThO_2 [2], and KBr [5]. For UO_2, a coincidence in temperatures of retarded release with the growth and annealing of bombardment-induced dislocation loops and small gas-filled bubbles has been shown [1]. Such a coincidence is indicated for α-Al_2O_3 as well, based on the present release data and on electron micrographic studies by Drum [21], and Wilks, Desport, and Bradley [22]: retarded gas release occurs between about 900 and 1600° C; the range of loop-annealing following reactor-

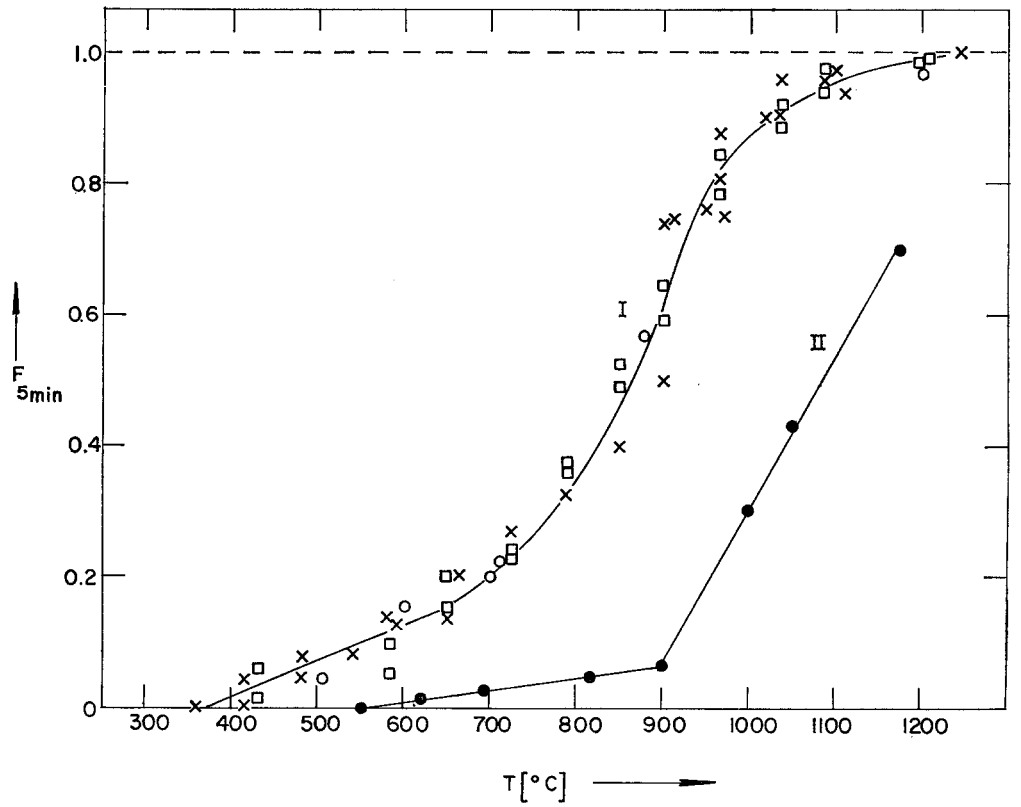

Figure 7 Release of xenon from U_3O_8 sinters and release of radon from U_3O_8 powders: □, Xe-125, 10^{11} ions/cm^2, sinter; ×, Xe-133, 4 × 10^{13} ions/cm^2, sinter; ○, Rn-222, 2 × 10^{10} ions/cm^2, powder; ●, Rn-222, 10^8 ions/cm^2, powder.

irradiation or argon-bombardment lies between about 800 and 1000° C to about 1500° C, and gas bubbles are present in argon-bombarded α-Al_2O_3 between about 900° C and at least about 1500° C.

Some indication of the existence of stage III, or *strong* trapping, in α-Al_2O_3 was obtained by following the release of gas which survived the amorphous/crystalline transition obtained in high-dose bombardments (high-temperature part of curves 1) or in the double bombardments of curve 5 of fig. 3. This gas was released only at temperatures well in excess of those of normal or retarded release (curves 2 to 4), implying that stage III release in α-Al_2O_3 starts at about 1400 to 1600° C. This high-temperature release cannot be due to evaporation, as evaporation is not significant below 1690 to 1750° C [8]. The shift of gas release towards high temperatures may rather be due to either formation of big bubbles or the existence of a polycrystalline surface layer. The amorphous/crystalline transition leads first to a polycrystalline state of the bombarded surface layer, the grain diameters (400 to 1000 Å) being comparable to the range of the gas. Thus, whereas, in ion-bombardment work with normal sinters, grain boundaries are not expected to influence gas release since their spacing (order of microns) is much bigger than the range of the gas, there might have been an effect in recrystallised Al_2O_3. This would indicate that gas, possibly precipitated into small bubbles, is *strongly* trapped at grain boundaries. Similar deductions have been reported [23] for fission xenon release in polycrystalline UO_2, and the interaction of bubbles with grain boundaries and dislocations has been observed in transmission electron microscopy (see, for example, references 4 and 24). If this explanation is correct, then grain boundaries would not be a path of fast diffusion as for self- or solute-diffusion but rather a site for strong trapping.

Within the experiments performed, no essential difference between the behaviour of various rare gases (Ar, Kr, Xe, Rn) and between different heating atmospheres (air, N_2, H_2) was observed. However, no new conclusion can be drawn from these observations: α-Al_2O_3 is probably un-

affected by the heating atmosphere in the used temperature range, and the comparison between different rare gases just implies a close similarity in their mobilities but does not allow one to draw a final conclusion yet as to the mechanism of stage II release.

The present work extends the knowledge on gas mobility in Al_2O_3. The results, together with previous studies [6-10, 20, 25, 26], yield a fairly clear picture of the various processes contributing to gas release from alumina. Stage II release, starting at roughly 0.55 $T_m \approx 1000°$ C, occurs at temperatures compatible with bulk self-diffusion [18, 19] and related processes such as annealing of dislocation loops [21, 22], with an ideal D_0 in the range 0.03 to 3 cm²/sec and a ΔH between 80 and 95 kcal/mole. Therefore, this release is regarded as involving normal volume diffusion of single gas atoms or mobility of small defect clusters. Release at temperatures well below those of stage II, designated as stage I, consists of at least three different processes [6, 9] which are attributed to different mechanisms. Surface proximity of the gas causing a reduction of the energy needed for defect migration, or motion of bombardment-induced point defects, or interstitial migration of the diffusing ion, as reported for xenon mobility in tungsten [27], have been tentatively suggested as causing the first two releases with activation enthalpies of 38 $\pm$ 2 and 55 $\pm$ 2 kcal/mole [9]. Recrystallisation of a phase change induced by high-dose bombardment was proven to coincide with the third release process at low temperatures [6]. This third process yielded an essentially single ΔH between 68 and 79 kcal/mole [6, 9]. Release at temperatures slightly above those of stage II is designated [1, 8] as "retarded release" or "*weak* trapping" and coincides in temperature with the annealing of dislocation loops and the growth of small bubbles [21, 22]. Release well above the temperature of stage II, designated as stage III, is thought to involve *strong* trapping owing to formation of big bubbles or interaction of gas (or bubbles) with grain boundaries (or dislocations),

6.2. Cr_2O_3 and Fe_2O_3

These two substances of the corundum type are expected to behave similarly to Al_2O_3. Normal volume diffusion (stage II) is expected to start at about 0.5 T_m ($\approx 650°$ C for Fe_2O_3; $\approx 850°$ C for Cr_2O_3) or at the temperatures of onset of self-diffusion: about 530 to 760° C for Cr in Cr_2O_3 [28, 29] and 905° C for O in Cr_2O_3 [30]; 785° C for Fe in Fe_2O_3 [31] and 685° C for O in Fe_2O_3 [32] (see table I of reference 10 for calculation of onset temperatures). Therefore, the release of curve 3 in fig. 4 and curves 3 and 4b in fig. 5 could well represent normal volume diffusion of the gas.

For Cr_2O_3, no difference was found for the two doses of 8×10^{10} and 4×10^{13} ions/cm², which is in favour of a bulk process. 20% of the gas, however, was retained to at least 1400° C, indicating the onset of a trapping effect. With increased dose, a phase change was started and, in analogy to Al_2O_3, most of the gas was released at low temperatures, in accordance with recent data by Kelly and Jech [10]. This release (curves 1 and 2 of fig. 4) will be discussed elsewhere.

With Fe_2O_3, a dose effect leading to a *decrease* in release temperatures was already implied for the lowest *xenon* dose, as seen by comparing curves 3 and 4b in fig. 5. Further increases in dose shifted the release gradually to lower temperatures, indicating a connection with the observed recrystallisation of structural damage. Whether or not the radon data (curve 4b) are representative for true volume diffusion cannot be decided as no lower dose could be used. However, the data and the ΔH are believed to be typical for stage II release. No indication of a high-temperature process was obtained for Fe_2O_3, since all gas was released below about 1200° C. This may be due to reduction of the oxide to Fe_3O_4 which proceeds at about this temperature (see also section 6.3).

Previous data on gas release from Fe_2O_3 or Cr_2O_3 [14, 25, 26, 33] showed very low activation energies at low temperatures, in accordance with the present data on Al_2O_3 and the interpretation of stage-I-type release. As with Al_2O_3 (fig. 2), a knee in the Arrhenius diagrams was observed at the temperatures for onset of stage II with higher activation enthalpies above the knee. This is in approximate agreement with the present results.

6.3. Rutile, TiO_2

Evidence of all three stages has been found in rutile, the dominance of each depending on the special conditions chosen for the experiment. Low-temperature release (stage I) was observed in all cases. It was dominant only at high bombardment doses and/or when samples were

reduced during the diffusion experiment (see also reference 6).

Stage II release is expected to start at roughly 0.5 T_m ($\approx 755°$ C). This is about the starting temperature of the second component of curves 1 and 2. Therefore, and because of the low gas concentration used ($\approx 10^5$ ions/cm^2), the radon data of curve 1 probably represent normal volume diffusion. Slight increases in dose lead to slight increases in release temperatures, indicating *weak* or temporary trapping (curve 2).* These results are similar to those found with Al_2O_3 (see fig. 3) where, at low doses, gas release is also compatible with volume diffusion, and where, at increased dose, a shift of the release to *higher* temperatures (retardation of the release) is observed, indicating weak trapping. At still higher doses, a phase change occurs, the reversal of which coincides with gas release at *low* temperatures.

Stage III, or *strong* trapping, was found with prereduced TiO_2 (curve 3): despite the low dose used, gas release rates were very small up to 1400° C, the highest temperature studied. Reduction of TiO_2 was shown by electron microscopy [34, 35] to produce stacking faults, dislocation loops, and vacancy clusters. Prereduced TiO_2 regains stoichiometry by heating in air at about 800° C. The differences between curves 3 and 2 show, therefore, two interesting features of gas release. In contrast to reduction of stoichiometric TiO_2 *during* diffusion (and oxidation of UO_2 during diffusion [36]), oxidation of TiO_{2-x} *during* diffusion does *not* enhance Xe release. Rather, release is shifted to *very high* temperatures. Even following oxidation to TiO_2, release is different from that from bombarded stoichiometric TiO_2. This might indicate an interaction of gas and *pre-existing* defects such as the above-mentioned stacking faults, dislocation loops, or vacancy clusters, which would be stabilised by the presence of the gas and would not anneal until *very high* temperatures were reached.

As with Al_2O_3, the mechanism for volume diffusion of the gas in TiO_2 is not completely clear as yet. The nature of the lattice disorder of TiO_2 has not been determined with certainty; both titanium interstitials (e.g. [12, 37, 38]) and oxygen vacancies (e.g. [39, 40]) have been suggested as being the dominant defects, the relative concentrations of which may depend on oxygen partial pressure (e.g. [41, 42]). However, the size of the rare gas atoms, together with the similarities of gas diffusion rates, oxygen self-diffusion [43], and sintering rates [44], all favour a mechanism for the mobility of the gas involving jumps *of* or *between* vacancies rather than an interstitial mechanism. The latter would be expected to dominate for smaller ions [38] and was shown, for the case of lithium, to be very fast and strongly anisotropic [45]. As with Al_2O_3, no final decision between the two more probable mechanisms can be made as yet. Again, doping experiments would be of questionable value, owing to the strong covalent contribution to the chemical bonding in TiO_2 (e.g. [46-48]).

The effect of reduction on gas release (i.e. the observed enhancement of diffusion associated with reduction *during* diffusion) is most pronounced at high or intermediate doses (4×10^{13} and 2×10^{16} ions/cm^2), whereas at the lower dose of 8×10^{10} Xe ions/cm^2 the effect is smaller. Actually, these latter data coincide with the radon data (very low dose of $\approx 10^5$ ions/cm^2) for annealing in air. This might indicate that the effect of reduction during diffusion is more one of enhancing release of *trapped* gas than release of *untrapped* gas. This would be in favour of a mechanism for volume diffusion of the gas involving small equilibrium vacancy clusters (jumps *of* vacancies) rather than single vacancies (jumps of the gas *between* equilibrium vacancies), since the concentration of single vacancies should be *directly* influenced by reduction, whereas the concentration of stoichiometric vacancy clusters would be largely unaffected by changes in one kind of vacancy only.

6.4. U_3O_8

Two different release curves were found for U_3O_8. Again, release from samples bombarded to a dose high enough to produce structural radiation damage occurred at lower temperatures than release following bombardment to a very low dose. Structural damage was observed for a dose of 8×10^{10} ions/cm^2 [6]. Since the release data for this dose coincided with those for the dose of 2×10^{10} ions/cm^2, this latter dose was probably high enough to

*The differences in bombardment geometry (powders for curve 1, single crystals representing a semi-infinite body for curve 2) are partly compensated by the lower energy for curve 2 (40 keV versus ≈ 85 keV for curve 1) and cannot explain the observed differences in release temperatures.

cause a phase change as well. Hence, U_3O_8 is more susceptible to disordering than other anisotropic oxides studied so far.

U_3O_8 decomposes even while being heated in air (e.g. [49-51]). Therefore, no temperature for the expected onset of volume diffusion can be calculated from the melting point. Furthermore, no attempt was made to look for structural radiation damage at the lowest dose used, $\approx 10^8$ ions/cm^2, as the samples employed were powders. However, following bombardment to this dose, isothermal release curves (fig. 1) followed the expected time-dependence for volume diffusion. Therefore, the corresponding data of fig. 7 might reflect undisturbed gas diffusion, and the calculated diffusion parameters $\Delta H = 89 \pm 8$ kcal/mole and $D_0 = 3 \times 10^{0 \pm 0.5}$ cm^2/sec may be assumed to be representative of the volume diffusion of rare gases in undamaged U_3O_8. However, owing to the slow decomposition of U_3O_8 during heating to temperatures in excess of about 600° C, a connection of gas release with the gradual reduction cannot be excluded. On the other hand, if such a connection exists, it will probably be impossible to measure rare-gas diffusion in stoichiometric U_3O_8.

The literature data [52-54] on the release of volatile fission products Kr, Xe, and I were obtained following reactor-irradiation. Hence, the samples were probably rendered quasi-amorphous before the start of the experiment and recrystallised during the experiment. Therefore, the observed diffusion constants (ΔH between 17 and 40 kcal/mole, D_0 between 10^{-11} and 10^{-4} cm^2/sec) are as expected and were found to be low and thus not typical for volume diffusion.

7. Conclusions and Summary

The present work shows the existence of different release processes for rare gases in the five anisotropic oxides, Al_2O_3, Cr_2O_3, Fe_2O_3, TiO_2, and U_3O_8. Release compatible with normal volume diffusion started at about 0.5 T_m (T_m = melting point on the absolute temperature scale), yielded D_0 values within the "ideal" range of about $3 \times 10^{-1 \pm 1}$ cm^2/sec, and gave activation enthalpies (in kcal/mole) of $\geqslant 85$ for Al_2O_3, 73 ± 5 for Cr_2O_3, 68 ± 5 for Fe_2O_3, 78 ± 5 for TiO_2, and 85 ± 8 for U_3O_8.

At doses in between the low ones, for which unperturbed volume diffusion was assumed, and the high ones, for which structural damage was proven, a retardation in gas release was observed. This indicates a *weak* or temporary trapping of the gas, implying a weak interaction of the gas with other gas atoms (e.g. small bubbles) or with bombardment-induced defects (e.g. dislocation loops).

A shift of release to very high temperatures was observed in prereduced rutile and in damaged and recrystallised corundum. This indicated *strong* trapping of gas implying a strong interaction of gas atoms with other gas atoms (large bubbles), or with pre-existing defects (like vacancy clusters, stacking faults, or grain boundaries in a microcrystalline surface layer).

Acknowledgements

The above work was carried out during the tenure of a postdoctoral fellowship of the National Research Council, Ottawa, in the Chalk River Nuclear Laboratories. The author thanks the staff members of the Chemistry and Metallurgy Division for generous help and Dr R. Kelly (CCR Euratom, Ispra) for discussions.

References

1. HJ. MATZKE, *Nuclear Applications* **2** (1966) 131.
2. *Idem, J. Nucl. Matls.* **21** (1967) 190.
3. T. LAGERWALL, *Nukleonik* **6** (1964) 179.
4. HJ. MATZKE, unpublished results.
5. *Idem, Z. Naturforsch.* **22a** (1967) 507.
6. HJ. MATZKE and J. L. WHITTON, *Canad. J. Phys.* **44** (1966) 995.
7. R. KELLY and F. BROWN, *Acta Met.* **13** (1965) 169.
8. R. KELLY and HJ. MATZKE, *J. Nucl. Matls.* **17** (1965) 179.
9. C. JECH and R. KELLY, *ibid* **20** (1966) 269; *Proc. Brit. Ceram. Soc.* **9** (1967), in press.
10. *Idem, Proc. Brit. Ceram. Soc.* **9** (1967), in press.
11. M. E. STRAUMANIS, T. EJIMA, and W. J. JAMES, *Acta Cryst.* **14** (1961) 493.
12. R. N. BLUMENTHAL, thesis, Northwestern Univ., USA; *Diss. Abs.* **23** (1963) 4646.
13. R. N. BLUMENTHAL and D. H. WHITMORE, *J. Electrochem. Soc.* **110** (1963) 92.
14. R. LINDNER and HJ. MATZKE, *Z. Naturforsch.* **15a** (1960) 1082.
15. J. R. MACEWAN, *J. Amer. Ceram. Soc.* **45** (1962) 37.
16. R. KELLY and HJ. MATZKE, *J. Nucl. Matls.* **20** (1965) 171.
17. G. DI COLA and HJ. MATZKE, *Euratom Report* (1967), in press.
18. A. E. PALADINO and W. D. KINGERY, *J. Chem. Phys.* **37** (1962) 957.

19. Y. OISHI and W. D. KINGERY, *ibid* **33** (1960) 480.
20. D. L. MORRISON, R. H. BARNES, T. S. ELLEMAN, and D. N. SUNDERMAN, *US Report* BMI-1592; *J. Appl. Phys.* **35** (1964) 1616.
21. C. M. DRUM, *Phys. stat. sol.* **9** (1965) 635.
22. R. S. WILKS, J. DESPORT, and E. BRADLEY, *Proc. Brit. Ceram. Soc.* **7** (1966).
23. R. M. CARROLL, R. B. PEREZ, and O. SISMAN, *J. Amer. Ceram. Soc.* **48** (1965) 55.
24. A. D. WHAPHAM, *Nuclear Applications* **2** (1966) 123.
25. W. SCHRÖDER, *Z. Elecktrochem.* **52** (1948) 133 and 166.
26. J. N. GREGORY and S. MOORBATH, *Trans. Faraday Soc.* **47** (1951) 844.
27. J. A. DAVIES and P. JASPERGÅRD, *Canad. J. Phys.* **44** (1966) 1631.
28. R. LINDNER and Å. ÅKERSTRÖM, *Z. phys. Chem.* **6** (1956) 162.
29. W. C. HAGEL and A. U. SEYBOLT, *J. Electrochem. Soc.* **108** (1961) 1146.
30. W. C. HAGEL, *J. Amer. Ceram. Soc.* **48** (1965) 70.
31. R. LINDNER, *Arkiv Kemi* **4** (1952) 381.
32. W. C. HAGEL, *Trans. Met. Soc. AIME* **236** (1966) 179.
33. HJ. MATZKE, Ph.D. thesis, Technical University, Braunschweig (1964).
34. K. H. G. ASHBEE, R. E. SMALLMAN, and G. K. WILLIAMSON, *Proc. Roy. Soc. A* **276** (1963) 542.
35. A. EIKUM and R. E. SMALLMAN, *Phil. Mag.* **11** (1965) 627.
36. R. LINDNER and HJ. MATZKE, *Z. Naturforsch.* **13a** (1958) 794.
37. T. HURLEN, *Acta Chem. Scand.* **13** (1959) 365.
38. H. J. GERRITSEN and E. S. SABINSKY, *Phys. Rev.* **125** (1962) 1835.
39. R. G. BRECKENRIDGE and W. R. HOSLER, *ibid* **91** (1953) 739.
40. C. J. KARANE, *ibid* **133** (1964) A 1431.
41. P. F. CHESTER, *J. Appl. Phys. Suppl.* **32** (1961) 2233.
42. J. YAHIA, *Phys. Rev.* **130** (1963) 1711.
43. R. HAUL and G. DÜMBGEN, *J. Phys. Chem. Solids* **26** (1965) 1.
44. D. H. WHITMORE and T. KAWAI, *J. Amer. Ceram. Soc.* **45** (1962) 375.
45. O. W. JOHNSON, *Phys. Rev.* **136** (1964) A 284.
46. P. ZERFOSS, R. G. STOKES, and C. H. MOORE JR, *J. Chem. Phys.* **16** (1948) 1166.
47. F. A. GRANT, *Rev. Mod. Phys.* **31** (1959) 646.
48. W. A. BAUER, *Acta Cryst.* **9** (1956) 515.
49. W. BILTZ and H. MÜLLER, *Z. anorg. Chem.* **163** (1927) 257.
50. R. VON AMMON, *Nukleonik* **5** (1963) 274.
51. J. R. JOHNSON, *Amer. Ceram. Soc. Bull.* **36** (1957) 112.
52. R. LINDNER and HJ. MATZKE, *Z. Naturforsch.* **14a** (1959) 582 and 1074.
53. T. J. KENNETT and H. G. THODE, *Canad. J. Phys.* **38** (1960) 945.
54. L. STIEGLITZ, Ph.D. thesis, Technical University, München (1963).